

Available online at www.sciencedirect.com

ScienceDirect

Physics Procedia 76 (2015) 80 – 85

Physics

Procedia

The 17th International Conference on Luminescence and Optical Spectroscopy of Condensed Matter (ICL2014)

Luminescence Properties of $\text{Sr}_2\text{MgSi}_2\text{O}_7:\text{Eu}^{2+}, \text{Ce}^{3+}$ Phosphor by Solid State Reaction Method^aIshwar Prasad Sahu*, ^aD.P. Bisen, ^aNameeta Brahme, ^aLata Wanjari, ^bRaunak Tamrakar^aSchool of Studies in Physics and Astrophysics, Pt. Ravishankar Shukla University, Raipur (C.G.) Pin Code-492010, India^bDepartment of Applied Physics, Bhilai Institute of Technology (Seth Balkrishnan Memorial) Durg (C.G.) Pin Code - 491001, India**Abstract**

The $\text{Sr}_2\text{MgSi}_2\text{O}_7:\text{Eu}^{2+}, \text{Ce}^{3+}$ phosphor was prepared by solid state reaction method, boric acid (H_3BO_3) was added as flux. The phase structure of $\text{Sr}_2\text{MgSi}_2\text{O}_7:\text{Eu}^{2+}, \text{Ce}^{3+}$ phosphor was akermanite type structure which belongs to the tetragonal crystallography with space group $\text{P4}_2\text{1m}$, this structure is a member of the melilite group and forms layered compound. EDX and FTIR spectra confirm the present elements in $\text{Sr}_2\text{MgSi}_2\text{O}_7:\text{Eu}^{2+}, \text{Ce}^{3+}$ phosphor. Three peaks in excitation spectra were found at 253, 293, 325nm and corresponding emission peak was recorded at 465nm, belonging to the broad emission ascribed to the $4f^65d^1 \rightarrow 4f^7$ transition of Eu^{2+} . The ML intensity of prepared phosphor was increasing linearly with increases of mechanical load.

Keywords: $\text{Sr}_2\text{MgSi}_2\text{O}_7:\text{Eu}^{2+}, \text{Ce}^{3+}$; XRD; Melilite; Photoluminescence; Mechanoluminescence.

1. Introduction

Persistent luminescence has been among the most popular subjects of investigations in the storage phosphors field since the late 1990s. Alkaline earth aluminates doped with the Eu^{2+} and R^{3+} ions ($\text{MAl}_2\text{O}_4:\text{Eu}^{2+}, \text{R}^{3+}$; $\text{M}=\text{Ca}, \text{Sr}$; $\text{R}=\text{Nd}, \text{Dy}$) have been introduced as new commercial persistent luminescence materials to replace $\text{ZnS}:\text{Cu}, \text{Mn}, \text{Co}$. [1-3] The luminescence properties of the aluminates are degraded when exposed to water and hence their use in luminous paints as a pigment is limited. Generally in Eu^{2+} and Dy^{3+} co-doped systems, the Eu^{2+} is considered as activator and the Dy^{3+} to produce some traps for electrons or holes. [4-5] Recently, great attentions have been paid to investigate the compounds of the melilite group.

The melilites are a large group of compounds characterized by the general formula $\text{M}_2\text{T}^1\text{T}^2\text{X}_7$, where M is a large monovalent or divalent cation, T^1 is a small divalent or trivalent cation in tetrahedral, T^2 is also a small cation in the other tetrahedral and X is an anion. [6-9] Currently, the ML phenomenon has attracted more attention in melilite group because of its potential application for sensing structural damage, fractures, and deformation. Many efforts have been devoted to developing ML sensors due to their various applications such as visualization of stress, damage detection for air planes or cars. At the same time, the high stabilities, such as resistance of water, thermal stability, are also very important for the application of ML. [10-11] In order to search better silicate ML phosphors, we investigated the different alkaline earth ions on the ML color and intensity of europium and cerium doped $\text{M}_2\text{MgSi}_2\text{O}_7:\text{Eu}^{2+}, \text{Ce}^{3+}$; $\text{M}=\text{Ba}, \text{Sr}, \text{Ca}$ etc. [12]

In this paper, solid state reaction method is applied to prepare the europium doped and cerium co-doped di-strontium magnesium di-silicate ($\text{Sr}_2\text{MgSi}_2\text{O}_7:\text{Eu}^{2+}, \text{Ce}^{3+}$) phosphor. Structural characterizations are studied on the basis of XRD and EDX analysis. FTIR (Fourier transform infrared) spectra were applied to investigate the qualitative analysis of the elements present in the prepared phosphor on the basis of different vibration bands.

* Corresponding author. Tel.: +919926993644;

E-mail address: ishwarprasad1986@gmail.com.

Luminescence properties were also investigated on the basis of photoluminescence (PL) and mechanoluminescence (ML) properties. In particular, the relation between ML intensity and impact velocity is close to linearity, which suggests that this phosphor can be used as sensors to detect the stress of an object.

2. Experimental Details

2.1 Material Preparation

The europium doped and cerium co-doped di-calcium magnesium di-silicate ($\text{Sr}_2\text{MgSi}_2\text{O}_7:\text{Eu}^{2+},\text{Ce}^{3+}$) phosphor was prepared by the high temperature solid state reaction method. The raw materials are strontium carbonate [SrCO_3 (99.90%)], magnesium oxide [MgO (99.90%)], silicon di-oxide [SiO_2 (99.90%)], europium oxide [Eu_2O_3 (99.99%)] and cerium oxide [Ce_2O_3 (99.99%)], all of analytical purity, were employed in this experiment. Boric acid [H_3BO_3 (99.99%)] was added as flux. Initially, the raw powders were weighed according to the nominal compositions of $\text{Sr}_2\text{MgSi}_2\text{O}_7:\text{Eu}^{2+}, \text{Ce}^{3+}$. Then the powders were mixed and milled thoroughly for 2 hour using the mortar and pestle. The grinded sample were placed in an alumina crucible and subsequently fired at 1250°C for 3 hour in a weak reducing atmosphere. The weak reducing atmospheres are generated with the help of activated charcoal. The work of reducing atmosphere is to convert Eu^{3+} to Eu^{2+} . At last the nominal compounds were obtained after the cooling down.

2.2 Characterization Techniques

The XRD pattern has been obtained from Bruker D8 Advanced X-ray powder diffractometer using $\text{CuK}\alpha$ radiation and the data were collected over the 2θ range 10° - 80° . Energy dispersive x-ray spectroscopy (EDX) was used for the elemental analysis of the prepared phosphor. FTIR spectra were recorded with the help of IR Prestige-21 by SHIMADZU for investigating the finger print region (1400 – 400 cm^{-1}) as well as the functional groups (4000 – 1400 cm^{-1}) of prepared phosphor in middle infrared region (4000 – 400 cm^{-1}) by mixing the sample with potassium bromide (KBr). The Photoluminescence (PL) spectra were recorded by RF 5301 PC Spectrofluorophotometer by SHIMADZU using the xenon lamp as excitation source. The Mechanoluminescence (ML) was monitored by a homemade setup having RCA 931 photomultiplier tube positioned below the lucite plate and connected to a storage oscilloscope (Scientific 300 MHz, SM 340). All measurements were carried out at room temperature.

3. Results and Discussions:

3.1. XRD Analysis:

In order to determine the phase structure, powder XRD analysis has been carried out. The typical XRD patterns of $\text{Sr}_2\text{MgSi}_2\text{O}_7:\text{Eu}^{2+}, \text{Ce}^{3+}$ phosphor with the calculated XRD pattern are shown in Fig. 1.

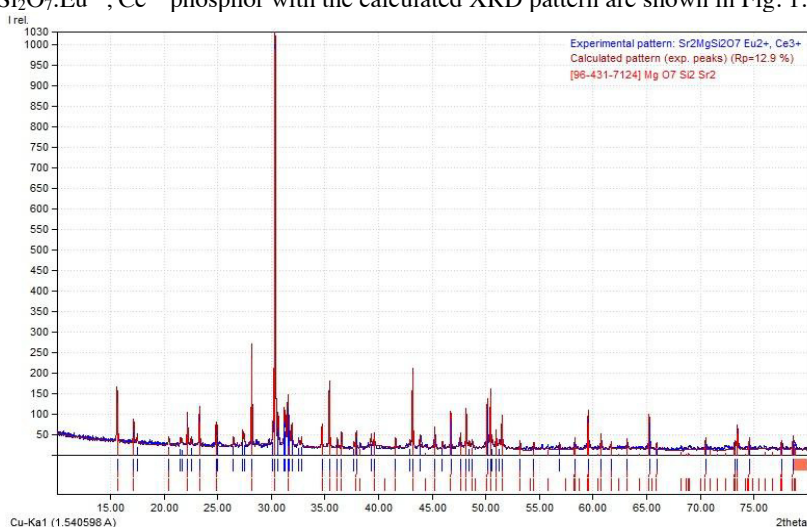


Fig. 1 X-ray diffraction patterns of $\text{Sr}_2\text{MgSi}_2\text{O}_7:\text{Eu}^{2+}, \text{Ce}^{3+}$ phosphor

The position and intensity of diffraction peaks of the prepared $\text{Sr}_2\text{MgSi}_2\text{O}_7:\text{Eu}^{2+}, \text{Ce}^{3+}$ phosphor were matched and found to be consistent with the standard XRD pattern (COD card No. 96-431-7124) by MATCH 2 software. The figure of merit (FOM) while matching these was 0.9530 (95%) which illustrates that the phase of the prepared sample agrees with the standard pattern COD card No. 96-431-7124. In Fig. 1, it can be concluded that prepared samples are chemically and structurally $\text{Sr}_2\text{MgSi}_2\text{O}_7$ phosphor which belongs to the tetragonal crystallography with space group $P 4_2/m$, this structure is a member of the melilite group and forms a layered compound.

3.2. Energy Dispersive X-Ray Spectroscopy (EDX):

The composition of the powder sample has been measured using EDX. Energy dispersive x-ray spectroscopy (EDX) is a standard procedure for identifying and quantifying elemental composition of sample area as small as a few nanometers. The existence of europium (Eu) and cerium (Ce) in the phosphor is clear in their corresponding EDX spectra. Their appeared no other emissions apart from Sr, Mg, Si and O in $\text{Sr}_2\text{MgSi}_2\text{O}_7:\text{Eu}^{2+}, \text{Ce}^{3+}$ in the EDX spectra of the samples. In the spectrum intense peak are present which confirm the formation of $\text{Sr}_2\text{MgSi}_2\text{O}_7:\text{Eu}^{2+}, \text{Ce}^{3+}$ phosphor in fig. 2.

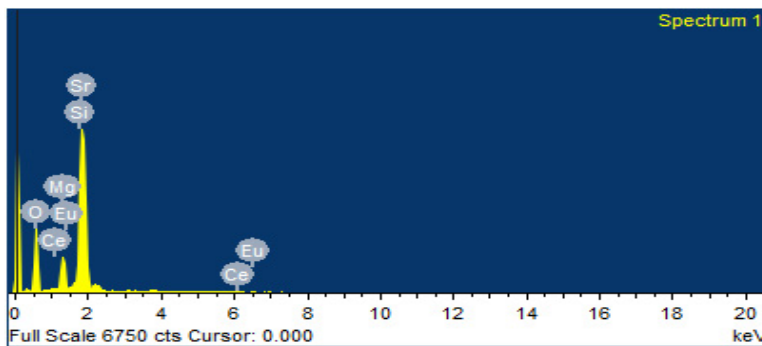
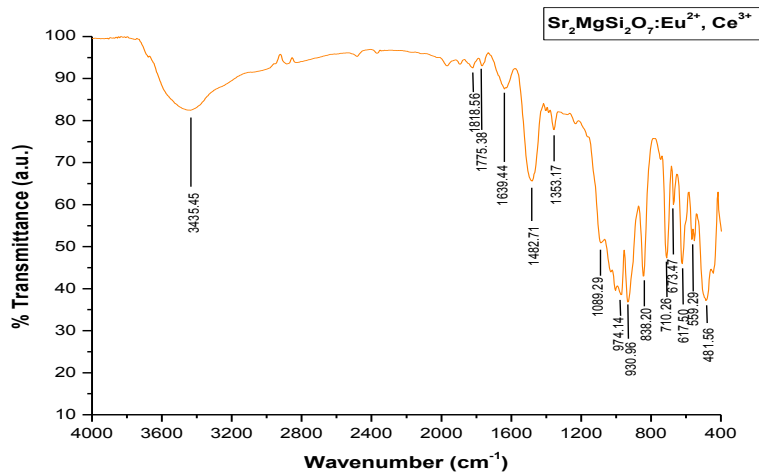


Fig. 2 EDX Spectra of $\text{Sr}_2\text{MgSi}_2\text{O}_7:\text{Eu}^{2+}, \text{Ce}^{3+}$ phosphor

3.3. Fourier Transform Infrared Spectra (FTIR):

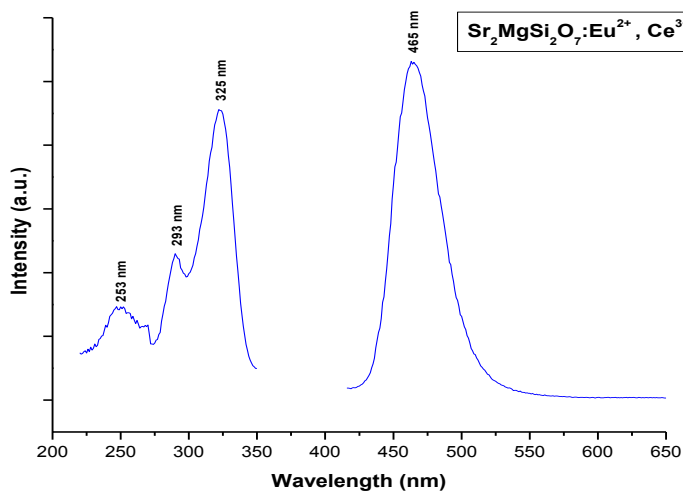
Fourier transform infrared spectroscopy (FTIR) has been widely used for the identification of organic and inorganic compounds. The infrared spectrum of an inorganic compound represents its physical properties. Spectroscopically, the middle infrared region ($4000\text{--}400\text{ cm}^{-1}$) is extremely useful for the study of organic and inorganic compounds. The wave-number of 3435.45 cm^{-1} is due to the O-H stretching mode. The O-H group around the 3435.45 cm^{-1} in sintered phosphor is might be due to presence of moisture through environment. The stretching around 1818.56 and 1775.38 cm^{-1} is assigned to CO_3^{2-} modes. The CO_3^{2-} modes (asymmetric stretching) around the 1800 to 1700 cm^{-1} in $\text{Sr}_2\text{MgSi}_2\text{O}_7:\text{Eu}^{2+}, \text{Ce}^{3+}$ phosphor is due the presence of carbonate (raw material). The free CO_3^{2-} ions has a D_{3h} symmetry (trigonal planar) and its spectrum is dominated by the band at 1800 to 1700 cm^{-1} . Eu^{2+} ions are expected to replace Sr^{2+} sites because the coordination number of Sr^{2+} ion is eight and that for Mg^{2+} ions and Si^{4+} ions is four. It's hard for Eu^{2+} ions to incorporate the tetrahedral $[\text{MgO}_4]$ or $[\text{SiO}_4]$ symmetry but it can easily incorporate octahedral $[\text{SrO}_6]$.

The vibration band of 1639.44 cm^{-1} are assigned due to the Mg^{2+} and bending of the sharp peaks in the region of 1482.71 cm^{-1} are assigned due to the bending of Sr^{2+} . The wave-number $1089.29, 974.14, 930.96, 838.20\text{ cm}^{-1}$ is due to the $(\text{Si-O}_b\text{-Si})$ and (Si-O_{nb}) stretching modes. The wave-number $710.26, 673.47, 617.50, 599.29\text{ cm}^{-1}$ are arises due to the (Si-O-Si) bending modes and the wave-number 481.56 cm^{-1} are based on the (Si-O-Si) bending modes as well as the Mg-O modes. In $\text{Sr}_2\text{MgSi}_2\text{O}_7:\text{Eu}^{2+}, \text{Ce}^{3+}$ phosphor; Mg^{2+} occupy the tetrahedral sites. FTIR spectra confirm the presence of elements in $\text{Sr}_2\text{MgSi}_2\text{O}_7:\text{Eu}^{2+}, \text{Ce}^{3+}$ phosphor. [13-16]

Fig. 3 FTIR Spectra of Sr₂MgSi₂O₇: Eu²⁺, Ce³⁺ phosphor

3.4. Photoluminescence (PL):

The excitation and emission spectra of Sr₂MgSi₂O₇:Eu²⁺, Ce³⁺ phosphor is shown in Fig. 4. The excitation spectrum was observed in the range of 200 to 350 nm and emission spectra were recorded in the range of 400 to 650 nm. The excitation broad band due to transitions of ⁸S_{7/2} (4f⁷) ground state to the excited state 4f⁶5d¹ [⁸S_{7/2} (4f⁷) → 4f⁶5d¹] configuration were observed under the ultra violet excitation. The excitation spectrum of the blue fluorescence (λ_{em} = 465 nm) shows three broad band's with their peaks at about 253, 293 and 325 nm, respectively, which are due to the crystal field splitting of the Eu²⁺ d orbital. Under the excitation of 325 nm, the emission spectrum shows a strong band with a peak at about 465 nm, which corresponds to 4f–5d transition of Eu²⁺ ions. The 5d energy level of Eu²⁺ and the lower level of 4f state overlap, so the electron of 4f state can be excited to 5d state.

Fig. 4 Excitation and emission spectra of Sr₂MgSi₂O₇: Eu²⁺, Ce³⁺ phosphor

The broad luminescence of Eu^{2+} is due to $4f^{65d^1-4f^7}$ transitions. It is known that the blue emission peaked at 465 nm corresponds to the transitions of ${}^4\text{F}_{9/2} \rightarrow {}^6\text{H}_{15/2}$, and this emission belongs to hypersensitive transition with $J=2$. The prepared $\text{Sr}_2\text{MgSi}_2\text{O}_7: \text{Eu}^{2+}, \text{Ce}^{3+}$ phosphor would emit blue light with peak at 465 nm. [17]

3.5 Mechanoluminescence (ML):

Mechanoluminescence (ML) is a type of luminescence induced by any mechanical action on solids. ML can be excited by compressing, stretching, bending, loading, shaking, cutting, cleaving, grinding, scratching, crushing or impulsive deformation of solids. In these ML studies, an impulsive deformation technique has been used for measurements. When a load is applied on to the sintered phosphor, initially the ML intensity increases with time, attains a peak value and then it decreases with time. During the deformation of a solid, a great number of physical processes may occur within very short time intervals, which may excite or stimulate the process of photon emission. Such a curve between the ML intensity and deformation and post-deformation time of a solid is known as the ML glow curve.

Fig. 5(a, A-D) shows that the characteristics curve between ML intensity versus time for different heights. The experiment was carried out for a fixed moving piston (400gm) dropped with different heights ($h = 20, 30, 40, 50$ cm). Every time for the ML measurement, the quantity of the powder sample were kept constant (8 mg). From Fig. 5 (a), when the moving piston is dropped onto the prepared $\text{Sr}_2\text{MgSi}_2\text{O}_7: \text{Eu}^{2+}, \text{Ce}^{3+}$ phosphor at different height, light is emitted. The light emission time is nearly 2 ms, when prepared material fractures. In these ML measurements, the maximum ML intensity has been obtained for the 50 cm dropping height of moving piston. Fig. 5(b) shows that the characteristics curve between ML intensity versus impact velocity. These figure shows that the ML intensity increases linearly with the increasing impact velocity of the moving piston $[\sqrt{2gh}]$ (where “g” is the acceleration due to gravity and “h” is the height through which the load is dropped freely)]. The ML intensity increases linearly with the increases the falling height of the moving piston; i.e., the ML intensity depends upon the impact velocity.

Furthermore the prepared $\text{Sr}_2\text{MgSi}_2\text{O}_7: \text{Eu}^{2+}, \text{Ce}^{3+}$ phosphor has a tetragonal structure with space group $\text{P}\bar{4}2_1\text{m}$, the previous researches have revealed that the crystal with this structure possesses piezo-electrification. When a mechanical stress, such as compress, friction, and striking, and so on, was applied on the sintered phosphors, piezo-electric field can be produced. Therefore, in such phosphor the ML excitation may be caused by the local piezoelectric field near the impurities and defects in the crystals.

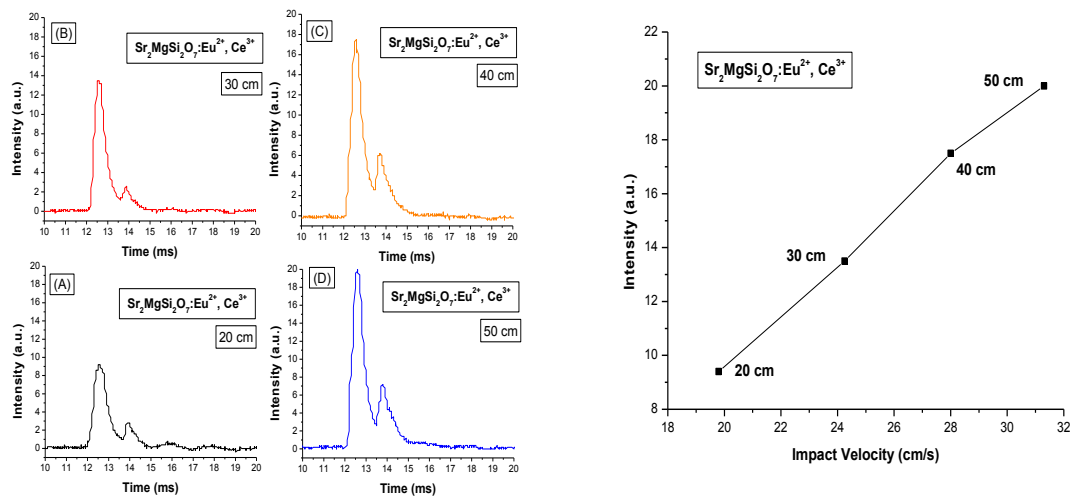


Fig. 5(a) ML intensity Vs time of $\text{Sr}_2\text{MgSi}_2\text{O}_7: \text{Eu}^{2+}, \text{Ce}^{3+}$ phosphor Fig. 5(b) ML intensity Vs impact velocity of $\text{Sr}_2\text{MgSi}_2\text{O}_7: \text{Eu}^{2+}, \text{Ce}^{3+}$ phosphor

During the impact of the sample, one of its newly created surfaces gets positively charged and the other surface of the crack gets negatively charged. Thus, an intense electric field of the order of $10^6 - 10^7$ Volt cm^{-1} is produced. Under such order of electric field, the ejected electrons from the negatively charged surface may be accelerated and subsequently their impact on the positively charged surfaces may excite the luminescence center. Thus, depending on the prevailing conditions, recombination luminescence may be produced. For the impact velocity v_0 , the impact pressure P_0 will be equals to, $P_0 = Zv_0$, where Z is a constant. With increasing value v_0 of the trap depth will decrease, therefore, for the trap depth beyond a particular pressure the traps will be unstable and they will be de-trapped, in which the number of de-trapped electrons will increases with the increasing impact velocity. Thus, the ML intensity will increase proportionally with increasing value of impact velocity (v_0). From fig. 5(b), it can be seen that the linear increase of compressive load can induce the increase of ML intensity, which shows the excellent linear relation. That is, the ML intensity of $\text{Sr}_2\text{MgSi}_2\text{O}_7:\text{Eu}^{2+}$, Ce^{3+} phosphor are linear proportional to the magnitude of the applied load, which suggests that this phosphor can be used as sensors to detect the stress of an object.[18]

4. Conclusions

The $\text{Sr}_2\text{MgSi}_2\text{O}_7:\text{Eu}^{2+}$, Ce^{3+} phosphor was synthesized by the high temperature solid state reaction method under weak reducing atmospheres. The radius of Eu^{2+} (1.12 Å) and Ce^{3+} (1.143 Å) are very close to that of Sr^{2+} (about 1.12 Å) rather than Mg^{2+} (0.65 Å) and Si^{4+} (0.41 Å). Therefore, the Eu^{2+} ions are expected to occupy the Sr^{2+} sites in the $\text{Sr}_2\text{MgSi}_2\text{O}_7$ host. The EDX and FTIR spectra confirm the presence of elements in $\text{Sr}_2\text{MgSi}_2\text{O}_7:\text{Eu}^{2+}$, Ce^{3+} phosphor. The prepared $\text{Sr}_2\text{MgSi}_2\text{O}_7:\text{Eu}^{2+}$, Ce^{3+} phosphor would emit blue light with peak at 465 nm corresponds to the transitions of ${}^4\text{F}_{9/2} \rightarrow {}^6\text{H}_{15/2}$. It can be seen that with increasing impact velocity, ML intensity also increases linearly i.e., the ML intensity of $\text{Sr}_2\text{MgSi}_2\text{O}_7:\text{Eu}^{2+}$, Ce^{3+} phosphor are lineally proportional to the magnitude of the impact velocity, which suggests that this phosphor can be used as sensors to detect the stress of an object.

Acknowledgment

“We are very much grateful to UGC-DAE Consortium for Scientific Research, Indore (M.P.) India, for the XRD Characterization and we are also very much thankful to Dr. Mukul Gupta for his co-operation”. We are very thankful to Dr. K.V.R. Murthy, Department of Applied physics, M.S. University Baroda, Vadodara, Gujarat, India for the photoluminescence study.

References

- [1] Y. Chen, B. Liu, M. Kirm, Z. Qi, C. Shi, M. True, S. Vielhauer, G. Zimmerer, J. Lumin. 118, (2006) 70–78.
- [2] W. Pan, G. Ning, X. Zhang, J. Wang, Y. Lin, J. Ye, J. Lumin. 128 (2008) 1975–1979.
- [3] Y. Hu, H. Wu, Y. Wang, C. Fu, Mater. Sci. Eng. B 172, (2010) 276 – 282.
- [4] Y. Lin, Z. Zhang, Z. Tang, X. Wang, J. Zhang, and Z. Zheng, J. Eur. Ceram. Soc., 21, (2001) 683.
- [5] B. Liu, C. Shi, M. Yin, L. Dong, Z. Xiao, J. Alloys Compd. 387 (2005) 65– 69.
- [6] I. P. Sahu, D. P. Bisen, N. Brahme, Res. Chem. Intermed, (2014). DOI 10.1007/s11164-014-1767-6.
- [7] Y. Murayama, N. Takeuchi, Y. Aoki, T. Matsuzawa, US Patent (1995) 5,424,006.
- [8] Y. Gong, Y. Wang, Z. Jiang, X. Xu, Y. Li, Mater. Res. Bull., 44 (2009) 1916–1919.
- [9] I. P. Sahu, D. P. Bisen, N. Brahme, R.K. Tamrakar, JRRAS. 8 (2015) 104-109.
- [10] I. P. Sahu, D. P. Bisen, N. Brahme, Lumin. J. Biol. Chem. Lumin. (2015). DOI 10.1002/bio.2869.
- [11] I. P. Sahu, D. P. Bisen, N. Brahme, L. Wanjari, R. K. Tamrakar, Res. Chem. Intermed, (2015). DOI:10.1007/s11164-015-1929-1.
- [12] R. D. Shannon, Acta Cryst, A 32, (1976), 751.
- [13] R. L. Frost, J. M. Bouzaid, B. J. Reddy, Polyhedron (2007) 262405.
- [14] I. P. Sahu, D. P. Bisen, N. Brahme, J. Biol. Chem. Lumin. (2014) <http://dx.doi.org/10.1002/bio.2771>.
- [15] P. Makreski, G. Jovanovski, B. Kaitner, A. Gajovic, T. Biljan, Vib. Spectrosc. (2007) 44162.
- [16] R. Caracas, X. Gonze, Phys. Rev. (2003) B 68184102-1.
- [17] H. Zhang, N. Terasaki, H. Yamada and C. N. Xu, Int. J. Mod Phys B, Vol. 23, Nos. 6 & 7 (2009) 1028-1033.
- [18] I. P. Sahu, D. P. Bisen, N. Brahme, Displays, 35 (2014) 279-286.